NeuroImage 59 (2012) 1085–1093

Contents lists available at SciVerse ScienceDirect

NeuroImage

journal homepage: www.elsevier.com/locate/ynimg

Anatomical insights into disrupted small-world networks in schizophrenia

Qifeng Wang [a], Tung-Ping Su [b,c], Yuan Zhou [d], Kun-Hsien Chou [e], I-Yun Chen [e], Tianzi Jiang [a,f,g,*], Ching-Po Lin [e,**]

[a] LIAMA Center for Computational Medicine, National Laboratory of Pattern Recognition, Institute of Automation, the Chinese Academy of Sciences, Beijing, China
[b] Department of Psychiatry, Taipei Veterans General Hospital, Taipei, Taiwan
[c] Department of Psychiatry, Collage of Medicine, National Yang-Ming University, Taipei, Taiwan
[d] Key Laboratory of Behavioral Science, Institute of Psychology, Chinese Academy of Sciences, Beijing, China
[e] Brain Connectivity Laboratory, Institute of Neuroscience, National Yang-Ming University, Taipei, Taiwan
[f] Key Laboratory for NeuroInformation of Ministry of Education, School of Life Science and Technology, University of Electronic Science and Technology of China, Chengdu, China
[g] The Queensland Brain Institute, The University of Queensland, Brisbane, Australia

ARTICLE INFO

Article history:
Received 17 March 2011
Revised 13 September 2011
Accepted 15 September 2011
Available online 22 September 2011

Keywords:
Anatomical connectivity
Diffusion tensor imaging
Graph theory
Small-world
Schizophrenia

ABSTRACT

Schizophrenia is characterized by lowered efficiency in distributed information processing, as indicated by research that identified a disrupted small-world functional network. However, whether the dysconnection manifested by the disrupted small-world functional network is reflected in underlying anatomical disruption in schizophrenia remains unresolved. This study examined the topological properties of human brain anatomical networks derived from diffusion tensor imaging in patients with schizophrenia and in healthy controls. We constructed the weighted brain anatomical network for each of 79 schizophrenia patients and for 96 age and gender matched healthy subjects using diffusion tensor tractography and calculated the topological properties of the networks using a graph theoretical method. The topological properties of the patients' anatomical networks were altered, in that global efficiency decreased but local efficiency remained unchanged. The deleterious effects of schizophrenia on network performance appear to be localized as reduced regional efficiency in hubs such as the frontal associative cortices, the paralimbic/limbic regions and a subcortical structure (the left putamen). Additionally, scores on the Positive and Negative Symptom Scale correlated negatively with efficient network properties in schizophrenia. These findings suggest that complex brain network analysis may potentially be used to detect an imaging biomarker for schizophrenia.

Introduction

Current pathophysiological theories about schizophrenia highlight the role of dysconnectivity; that is, the complex clinical presentations (positive symptoms, negative symptoms and cognition decline) of schizophrenia arise from abnormality in inter-regional interactions rather than from abnormality in a specific focal region (Andreasen et al., 1999; Bullmore et al., 1997; Friston, 1998; Stephan et al., 2006). The dysconnection concept can also be described as an alteration in the efficiency of information exchange between separate neuronal networks in the human brain (Boutillier et al., 2008), which functions as a large, sparse, and complex network with highly efficient information processing between spatially distinct brain areas (Sporns et al., 2004). Network analysis derived from graph theory has successfully characterized the underlying architectures of such a network (Stam and Reijneveld, 2007) and has found so-called "small-world" properties in the brain (Bullmore and Sporns, 2009; Salvador et al., 2005; Sporns et al., 2004). Small-world properties enable the cortical network to process global and local information with maximal efficiency at minimal cost (Achard and Bullmore, 2007). Using functional neuroimaging techniques, researchers have found that small-world properties are disrupted in patients with schizophrenia (Bassett et al., 2009; Liu et al., 2008; Micheloyannis et al., 2006). These findings provide further evidence for the dysconnection hypothesis of schizophrenia. The anatomical network in the multimodal cortices was found to be disorganized in schizophrenia when researchers considered inter-regional covariation between gray matter volumes as a proxy for connectivity (Bassett et al., 2008). This study hinted at a structural basis for the disrupted functional network but only provided indirect anatomical evidence because the connectivity matrix was estimated based on inter-regional correlations across subjects. Thus, a crucial question that remains unresolved is whether the dysconnection manifested by the disrupted small-world functional network in schizophrenia is the result of underlying structural disruptions.

* Correspondence to: T. Jiang, LIAMA Center for Computational Medicine, National Laboratory of Pattern Recognition, Institute of Automation, the Chinese Academy of Sciences, Beijing 100190, PR China. Fax: +86 10 62551993.
** Correspondence to: C.-P. Lin, 155 Li-Nong St., Sec. 2, Peitou, Taipei, 112, Taiwan. Fax: +886 2 28262285.
E-mail addresses: jiangtz@nlpr.ia.ac.cn (T. Jiang), chingpolin@gmail.com (C.-P. Lin).

1053-8119/$ – see front matter © 2011 Elsevier Inc. All rights reserved.
doi:10.1016/j.neuroimage.2011.09.035

Because diffusion MRI is advantageous for visualizing brain anatomical connectivity *in vivo*, it has been increasingly used to investigate the intrinsic topological properties of the human brain network. This method facilitates our understanding of brain organization and of its complex cooperating working mechanisms at the macroscopic scale. Hagmann et al. confirmed a small-world topology which is connected by dense cortico-cortical axonal pathways in the human cortical network (Hagmann et al., 2007), and further found the structural core of the anatomical network (Hagmann et al., 2008). Since these early studies, researchers using diffusion tensor imaging (DTI) have consistently found small-world topology in anatomical networks connected by white matter fibers in healthy volunteers (Gong et al., 2009a; Iturria-Medina et al., 2008; Li et al., 2009). These studies indicate that using DTI to investigate anatomical networks is feasible in disease conditions such as schizophrenia. Skudlarski et al. constructed separate functional and anatomical connectivity maps for 27 schizophrenia patients and 27 normal controls and reported reduced coherence between functional and structural modalities in patients compared with normal controls (Skudlarski et al., 2010). In addition, they also reported a significant correlation between brain connectivity and the positive symptom score on the Positive and Negative Symptom Scale (PANSS). However, this study did not mention any analysis of the network topological properties. Zalesky et al. constructed binary structural networks for 74 chronic schizophrenia patients and 32 control subjects using a deterministic white matter tracking algorithm, and reported widespread dysconnectivity in the white matter connectional architecture in the patients group (Zalesky et al., 2010). They found that intellectual performance was associated with brain efficiency in the control subjects but not in the patients. However, this study did not examine the relationship between clinical variables and topological properties. In another study, van den Heuvel et al. utilized DTI and the magnetic transfer imaging (MTR) technique to construct weighted structural networks for 40 schizophrenia patients and 40 healthy controls and reported a reduced global efficiency of the frontal, temporal, and occipital brain regions in schizophrenia (van den Heuvel et al., 2010). They also examined the correlation between the PANSS and network properties but found no significant results. The results of these recent studies indicated that the structural brain network revealed by DTI is disrupted in schizophrenia. However, independent studies with larger samples are necessary to verify this inference. Additionally, correlations between clinical findings and disrupted structural networks in schizophrenia remain inconsistent (Skudlarski et al., 2010; van den Heuvel et al., 2010) and require further investigations.

Our goal for this study was to use DTI to detect abnormalities in the global architecture of the anatomical connectivity patterns in schizophrenia from the perspective of the brain network. Our focus was on network efficiency, which is defined to measure how well information propagates over the network (Latora and Marchiori, 2003). Furthermore, we attempted to find clinical correlations to the abnormalities we found in the topology of the anatomical network in patients with schizophrenia.

Materials and methods

Subjects

Some of the subjects included in this work were used in a previous study (Bai et al., 2009). However, in the current study additional subjects who had the same MRI scan parameters were recruited. We recruited 79 patients from the Psychiatric Department Outpatient Clinic and Day Care Unit at the Taipei Veterans General Hospital who met the Diagnostic and Statistical Manual of Mental Disorders, Fourth Edition (DSM-IV) criteria for schizophrenia. Subjects were excluded if they had other Axis I psychiatric diagnoses, serious neurologic or endocrine disorders, any medical condition or treatment known to affect the brain, alcohol/substance misuse related disorders, or mental retardation as defined by DSM-IV criteria. Before scanning, the patients' schizophrenia symptoms were rated by trained and experienced psychiatrists using PANSS (Kay et al., 1987) to rate the severity of psychopathology and the 17-item Hamilton Depression Rating Scale (HDRS) (Hamilton, 1960) to evaluate the depressive symptoms.

We recruited 96 healthy subjects (normal control group) via advertisement. The healthy subjects were interviewed using the Mini-International Neuropsychiatric Interview to confirm that they had no previous history of neurologic or psychiatric illness, and all had normal brain structure confirmed by MRI scans. The exclusion criteria were the same as those for the patient group.

The two groups were significantly similar in terms of gender composition, age, and brain size (Table 1).

Ethics statement

All procedures were approved by the institutional review board of Taipei Veterans General Hospital. Written informed consent was obtained from all subjects.

MRI data acquisition

All MR examinations were performed on a 1.5 T MR system (Excite II; GE Medical Systems, Milwaukee, WI, USA) equipped with an 8-channel head coil in TPE-VGH. To diminish motion artifacts generated during the scan, the subject's head was immobilized with cushions inside the coil after the alignment. One hundred twenty-four contiguous axial T1-weighted images (slice thickness = 1.5 mm) were acquired parallel to the anterior–posterior commissure (AC-PC) through the whole head by applying a three-dimensional fluid-attenuated inversion-recovery fast spoiled-gradient recalled echo (FLAIRFSPGR) acquisition sequence (TR = 8.548 ms, TE = 1.836 ms, TI = 400 ms, flip angle = 15°, field of view = 26 × 26 cm, matrix size = 256 × 256) to aid in the localization of differences in fractional anisotropy (Madden et al., 2004). Fourteen diffusion tensor imaging volumes were obtained for each subject, including thirteen volumes with diffusion gradients applied along thirteen non-collinear directions ($b = 900$ s/mm^2) and one volume without diffusion weighting ($b = 0$). In order to obtain coverage of the entire brain, each volume consisted of 70 contiguous axial slices (slice thickness = 2.2 mm) acquired parallel to the AC-PC by using a single shot spin-echo echo planar imaging (EPI) sequence (TR = 17,000 ms, TE = 68.9 ms, number of excitation = 6, field of view = 26 cm^2, matrix size = 128 × 128).

Table 1
Demographic and clinical details (mean ± SD).

	NC (N = 96)	SCZ (N = 79)	P-value
Gender (male/female)	48/48	39/40	0.934[a]
Age (years)	37 ± 13	37 ± 11	0.986[b]
Brain size (voxels)	174,650 ± 16,660	172,158 ± 15,355	0.309[b]
Duration (years)	____	10 ± 9	____
PANSS_p	____	13 ± 5	____
PANSS_n	____	14 ± 4	____
PANSS_t	____	59 ± 16	____

Abbreviations: SD, standard deviation; NC, normal controls; SCZ, schizophrenia; PANSS, Positive and Negative Symptom Scale; PANSS_p, positive scale score obtained from PANSS; PANSS_n, negative scale score obtained from PANSS; PANSS_t, PANSS total score.

[a] The p value was obtained using the Pearson Chi-square.

[b] The p value was obtained by a two-tailed two-sample *t*-test.

Preprocessing

For the diffusion-weighted images, simple head motion and eddy current distortion were corrected using FMRIB's Diffusion Toolbox (FSL 4.1; http://www.fmrib.ox.ac.uk/fsl). After correction, the six independent components of the diffusion tensor, the corresponding FA and eigenvectors were calculated using an in-house software named DTI Tracking (http://www.ccm.org.cn/). The T1-weighted image of each subject was co-registered to the subject's non-diffusion-weighted image ($b=0$ s/mm^2) using the SPM2 package (http://www.fil.ion.ucl.ac.uk/spm), resulting in a co-registered T1 image in native DTI space.

Construction of weighted brain anatomical connectivity networks

Definition of network node

We used the automated anatomical labeling (*AAL*) template (Tzourio-Mazoyer et al., 2002) available with the MRIcro software (http://www.sph.sc.edu/comd/rorden/mricro.html) to segment the entire cerebral cortex of each subject into 90 regions (45 for each hemisphere) with the cerebellum excluded. Each brain region represented a node of the final anatomical network. Each individual co-registered T1 image was normalized to the SPM2 T1 template in Montreal Neurological Institute (MNI) space. The resulting transformation matrix was then inverted and further used to warp the *AAL* template from the MNI space to the diffusion MRI native space, in which the discrete labeling values were preserved, using a nearest-neighbor interpolation method.

Definition of network edge

We implemented a deterministic streamline tracking algorithm (Mori et al., 1999) to perform fiber tracking. The tracking procedure ended at voxels with an FA value of less than 0.15 or when the angle between adjacent steps was greater than 45° (Li et al., 2009; Thottakara et al., 2006). Two *AAL* regions could be considered to be connected if the two end points of the reconstructed fiber bundles were located in these two regions (Gong et al., 2009a; Li et al., 2009).

The inverse of the number (N_{ij}) of connections between the two regions was employed to weigh the edge:

$$W_{ij}=\begin{cases}\dfrac{1}{N_{ij}} & \text{if}\left(N_{ij}\geq T\right)\\ 0 & \text{otherwise}\end{cases}.$$

Under this definition, w_{ij} is thought to be inversely related to the degree to which nodes i and j are connected anatomically; that is, the larger the w_{ij} (corresponding to a smaller N_{ij}), the weaker the connectivity strength between these two nodes. In other words, w_{ij} is proportional to the distance between two brain regions. However, note that distance here does not correspond to the physical distance between cortical regions in Euclidean space but to a quantification of the connectivity strength. Two regions that are linked by fewer fiber bundles are considered distant and correspond to a higher w_{ij}, which is similar to the definition used in previous studies (Achard and Bullmore, 2007; Gong et al., 2009b). Because false-positive connections could result from using this, we utilized a series of threshold values (T, from 1 to 10) for the number of existing fibers to examine the robustness of our construction method, that is, two regions linked with fewer than T fibers were treated as disconnected. The selected threshold values maintained the average size of the largest connected component at 90 across all subjects, meaning that the networks of the majority of subjects were fully connected at each threshold value (Table S1 in the Supplementary materials).

Graph theoretical analyses of the weighted network properties

Network properties definition

The topological properties utilized in our current study can be described as follows:

G is used to denote the whole weighted network; whereas G_i is defined as the subgraph of node i, which is constructed by its direct neighbor nodes and the edges linking these neighbor nodes.

N is used to represent the total number of nodes in the network.

The cost of a connection edge is proportional to its distance (weight), and the overall cost of a network is defined as the sum of the weights:

$$\text{cost}=\sum_{i\neq j\in G} w_{ij}.$$

The shortest path length between nodes i and j, L_{ij}, is defined as the length of a path from node i to node j in which the sum of the weights of its constituent edges is minimized.

The mean shortest path length of node i is computed as the average shortest path length between node i and all other nodes in the network:

$$L_i=\frac{1}{N-1}\sum_{j\in G, i\neq j} L_{ij}.$$

The characteristic path length of the network is the average of the shortest path lengths across all nodes:

$$L_p=\frac{1}{N}\sum_{i\in G} L_i.$$

The global efficiency of the network, E_{glob}, is defined as the inverse of the harmonic mean of the shortest path lengths between each pair of nodes:

$$E_{glob}=\frac{1}{N(N-1)}\sum_{i,j\in G, i\neq j}\frac{1}{L_{ij}}$$

E_{glob} measures the global efficiency of parallel information transfer in the network (Latora and Marchiori, 2001).

The regional efficiency of node i, $E_{reg(i)}$, $i=1,2,\ldots,90$, is defined as the inverse of the harmonic mean of L_{ij} between node i and all other nodes in the network (Achard and Bullmore, 2007):

$$E_{reg(i)}=\frac{1}{N-1}\sum_{i,j\in G, i\neq j}\frac{1}{L_{ij}}.$$

This measure quantifies the importance of each node for communication within the network (Gong et al., 2009b).

The local efficiency of node i, $E_{loc(i)}$, $i=1,2,\ldots,90$, is calculated as the global efficiency of G_i:

$$E_{loc(i)}=E_{glob}(G_i).$$

The local efficiency measures the fault tolerance of the network, indicating how well the information is communicated between the neighbors of a given node when the node is removed (Achard and Bullmore, 2007).

The local efficiency of the entire network, E_{loc}, is defined as the average of the local efficiencies across all nodes in the network:

$$E_{loc}=\frac{1}{N}\sum_{i\in G} E_{loc(i)}.$$

Evaluation of the small-world properties

The "small-world" concept, in which networks are characterized by a characteristic path length L less than that in a regular lattice and a clustering coefficient C greater than that in a random graph, was originally proposed in a study of binary networks (Watts and Strogatz, 1998). However, weighted networks have been demonstrated to be better suited for characterizing real world network topology, and E_{glob} and E_{loc} have been found to be suitable scales for characterizing the "small-world" properties of weighted networks (Achard and Bullmore, 2007; Latora and Marchiori, 2001). Fundamentally, $1/L$ measures the efficiency of a sequential system, whereas E measures the efficiency of parallel systems, in which all the nodes in the networks concurrently exchange packets of information. Characteristic path length is hypersensitive to local changes, whereas efficiency is more robust to link lesions or malfunctions. For example, in the case of a fully connected network, if one node in the network becomes isolated as the result of some accident, the mean shortest path length of the whole network tends to infinity, whereas the mean global efficiency is only slightly diminished (Achard and Bullmore, 2007). In general, the network would still work well even though localized damage has occurred; hence efficiency is more appropriate for measuring the performance of a parallel system, such as the human brain. Practically speaking, a weighted network can be categorized as small-world if E_{glob} is slightly less than, but E_{loc} is much greater than, a matched random network (Achard and Bullmore, 2007; Gong et al., 2009b). Here we followed the procedure used by Gong et al. (2009b) to evaluate the small-world properties. Specifically, we generated 100 random networks for each subject's network using a Markov-chain algorithm while retaining the weight of each edge in order to preserve the weight distribution of the entire network. Then we calculated E_{glob} and E_{loc} across these random networks and compared them with the properties of the real networks (see results).

Statistical analyses

A general linear model (GLM) was used to test for differences in the network properties (E_{glob}, E_{loc} and regional efficiency) between the schizophrenic patients and the healthy subjects. The gender, age and brain size of the subjects were included as covariates in order to exclude their potential effect (Gong et al., 2009b). In addition, partial correlation analyses between these properties and the clinical measures, including the PANSS total score (PANSS_t), the score on the PANSS positive subscale (PANSS_p), the score on the PANSS negative subscale (PANSS_n), and the duration of illness, were performed across the patients while controlling for age, gender, brain size and HDRS. All of the above statistical analyses were performed using SPSS 13.0 software. The threshold value for establishing significance was set at $p<0.05$ when performing the global properties analyses (E_{glob} and E_{loc}). However, when performing the nodal analysis (i.e. regional efficiency of each node), a threshold of $p<0.01$ (uncorrected for multiple comparisons) was used.

Results

To explore the dependence of our results on the choice of threshold, we reproduced the construction of weighted networks using 10 different threshold values (from 1 to 10). Similar results were consistently observed, suggesting that our findings are relatively robust (Tables S2, S3 in the Supplementary materials).

Small-world properties of the anatomical networks

As expected, the anatomical networks became sparser as the fiber number threshold increased (Fig. S1). The network sparsity range (12%–24%) was similar to that found in various other studies (Achard and Bullmore, 2007; Gong et al., 2009b; Li et al., 2009; Liu et al., 2008). The E_{glob} and E_{loc} of the anatomical networks as well as of the matched random networks were demonstrated to be a function of the fiber number threshold in both the normal control group and the schizophrenia group (Fig. 1A, B). Compared with the matched random networks, the real anatomical networks had a little lower global efficiency but a much higher local efficiency over the entire range of the connectivity thresholds. This pattern is characteristic of the small-world behavior of weighted brain networks (Achard and Bullmore, 2007; Gong et al., 2009b) and indicates that the anatomical networks are very efficient with respect to both global and local information transfer.

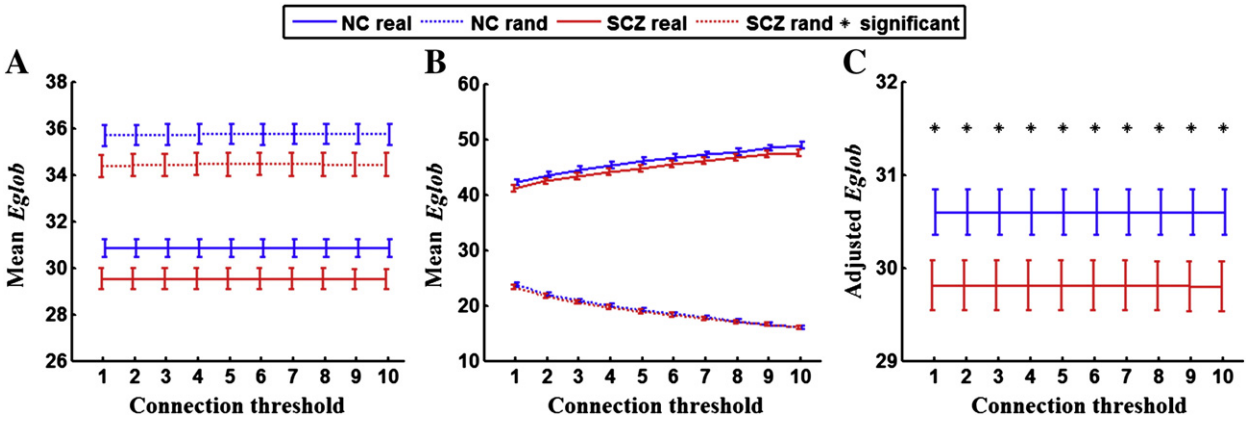

Fig. 1. Efficiency properties of the weighted anatomical network of the normal control group (N = 96) and the schizophrenia group (N = 79). The weighted network has a similar global efficiency (A) but a much higher local efficiency (B) than the matched random network over the entire sparsity range, indicating its small-world character. (C) The adjusted mean global efficiency of the normal control group is significantly higher than that of the schizophrenia group. The result was calculated using a general linear model after adjusting for the effects of gender, age and brain size. The solid line represents the results of the real network; the dashed line represents the results of the random network. The blue line represents the results of the normal controls; the red line represents the results of the schizophrenia patients. The black star represents that there was a significant difference under the current threshold. The significance threshold was set at $p<0.05$. Abbreviations: E_{glob}, the global efficiency of the network; E_{loc}, the local efficiency of the network; the words "real" and "rand" in the above figure indicate real anatomical networks and matched random networks respectively; for the other abbreviations please see Table 1. The error bars represent the standard error of the network efficiency across subjects.

Altered global topological properties of the anatomical networks in schizophrenia

Using a GLM statistical analysis, we found that, after factoring out the effects of age, gender and brain size, E_{glob} was significantly larger in the healthy group than in the schizophrenia patients over the entire threshold range (Fig. 1C, and Table S2 in the Supplementary materials). No significant difference in E_{loc} was found between the two groups, although E_{loc} showed a trend toward a decrease in the schizophrenia group compared to the normal group. We further examined the mean edge number and mean cost of the networks in both the two groups, without detecting any significant group differences.

Regional efficiency differences of individual nodes

The regional efficiency of each node is a measure of its connectivity to all the other nodes of the network (Achard and Bullmore, 2007). Nodes with high regional efficiencies can be regarded as "hubs". The 90 regional nodes were ranked in descending order according to their regional efficiency (see Fig. 2 and Table S4 in the Supplementary materials). In general, most of the nodes with a high regional efficiency belonged to the association cortex or to the paralimbic/limbic regions in both the schizophrenia and control groups. Compared with normal controls, a decreased regional efficiency in schizophrenia occurred primarily in regions of the frontal associative cortex, the paralimbic/limbic regions, and the subcortical structures (Fig. 3 and Table 2), indicating that inter-regional connectivity between these brain regions may be disrupted in schizophrenia.

Relationship between the topological measurements and the clinical PANSS

Since the statistical results showed similar trends across all thresholds without loss of generality, from here on we will utilize a mid-range threshold of 6. We found that E_{glob} was significantly negatively correlated with the PANSS_p ($p=0.017$, partial correlation coefficient (pcc) $=-0.308$), PANSS_n ($p=0.007$, pcc $=-0.346$) and PANSS_t ($p=0.006$, pcc $=-0.355$)) and that E_{loc} was also significantly negatively correlated with the PANSS_p ($p=0.042$, pcc $=-0.266$), PANSS_n ($p=0.006$, pcc $=-0.353$) and PANSS_t ($p=0.008$, pcc $=-0.340$). We show this pattern at a typical threshold $T=6$ in Fig. 4. Additionally, regional efficiencies in the frontal association cortex, paralimbic/limbic regions and subcortical structures were found to be negatively correlated with the PANSS scores (Table S5 in the Supplementary materials).

Discussion

This study used deterministic tractography based on diffusion MRI to demonstrate deficits in the macroscale anatomical brain networks in patients with schizophrenia. Zalesky et al. (2010) and van den Heuvel et al. (2010) also utilized the *AAL* template and a deterministic tracking method to construct a brain connectivity network and reported the presence of disrupted network topology in schizophrenia. However, the work reported in this current study has some methodology differences from these previous studies. Specifically, van den Heuvel et al.'s work was mainly concerned with the

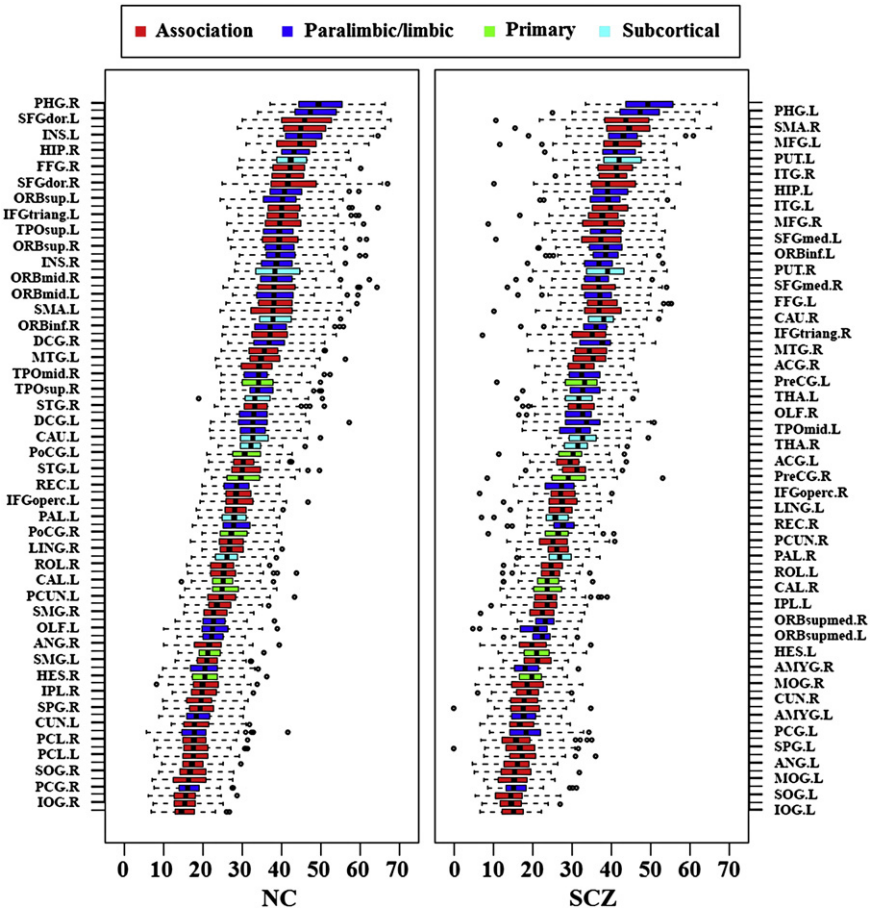

Fig. 2. The integrated regional efficiency for all regions in the normal group and in the patient group. The brain regions were ranked in the order of descending mean integrated regional efficiency across subjects within the healthy group. Abbreviations: please see Table S4 in the Supplementary materials.

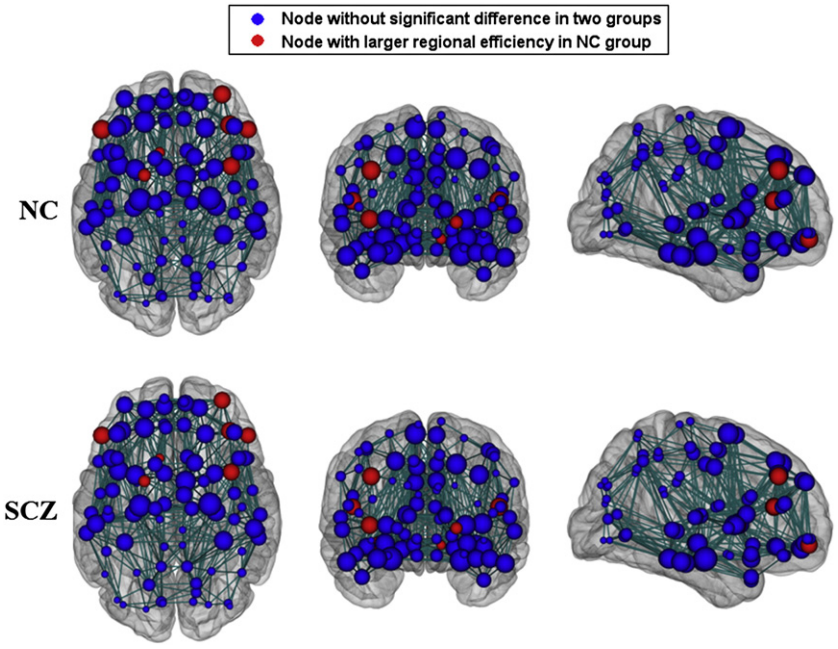

Fig. 3. 3D anatomical representation of the integrated regional efficiency for all brain regions of the normal control group (N = 96) and of the schizophrenia group (N = 79). The vertexes correspond to the 90 *AAL* regions (please see Table S4 in the Supplementary materials). The size of the vertices is proportional to the mean regional efficiency. The lines correspond to the connections between corresponding pairs of brain regions and indicate that at least half of the subjects showed a connection in each group. The significance threshold was set at $p<0.01$, uncorrected. Abbreviations: please see Table 2.

characteristic path length and clustering coefficient properties. As we discussed above, the efficiency property is a more sophisticated measure than the characteristic path length and clustering coefficient in brain connectivity network analyses (van den Heuvel et al., 2010). Additionally, Zalesky et al. (2010) investigated a binary network whereas we primarily considered a weighted network. Our main findings are (1) that global topological properties, as indicated by small-world parameters, were disturbed in schizophrenia, (2) that the regional efficiency of the prefrontal cortex and the paralimbic/limbic regions was affected in schizophrenia patients, and (3) that the topological measurements of the efficient small-world brain anatomical networks were correlated with clinical variables in schizophrenia. Taken together, our findings suggest that the global architecture of the anatomical connectivity patterns is altered in schizophrenia, which is in accord with findings from previous studies (van den Heuvel et al., 2010; Zalesky et al., 2010). These findings thus provide new anatomical evidence for core aspects of the pathophysiology of schizophrenia and also suggest that deficits in the coordination of macroscale brain networks underlie the abnormal brain function and clinical symptoms observed in schizophrenia.

Table 2
Brain regions showing significant differences in adjusted regional efficiency between the normal control group (N = 96) and the schizophrenia group (N = 79) ($p<0.01$, uncorrected).

Class	Brain region	Mean value (SD)		P-value[a]
		NC (N = 96)	SCZ (N = 79)	
Association	MFG.R	40.33 (5.51)	38.14 (5.50)	0.010
	IFGtriang.L	40.55 (5.32)	38.15 (5.32)	0.004
	IFGtriang.R	37.18 (4.79)	34.74 (4.79)	0.001
Paralimbic/limbic	ORBmid.R	38.35 (4.52)	36.51 (4.52)	0.008
	OLF.L	22.71 (4.59)	20.60 (4.59)	0.003
	INS.R	38.83 (3.92)	37.22 (3.93)	0.008
Subcortical	PAL.L	27.76 (3.70)	26.18 (3.72)	0.005

Abbreviations: MFG.R, Right middle frontal gyrus; IFGtriang.L, left inferior frontal gyrus, triangular part; IFGtriang.R, right inferior frontal gyrus, triangular part; ORBmid.R, right middle frontal gyrus, orbital part; OLF.L, left olfactory cortex; INS.R, right insula; PAL.L, left lenticular nucleus, pallidum; the others, please see Table 1.

[a] All results here were calculated using a general linear model after adjusting for the effects of gender, age and brain size.

Small-worldness is a fundamental principle of the structural and functional organization of complex brain networks (Bullmore and Sporns, 2009). Our finding of disrupted global topological structures in the anatomical network of schizophrenia is concordant with some recent network studies of schizophrenia. Electroencephalography (Micheloyannis et al., 2006), magnetoencephalography (Bassett et al., 2009), and functional MRI (Liu et al., 2008) have revealed disrupted and less efficient small-worldness in functional networks in schizophrenia. By measuring inter-regional correlations in the gray matter volume, disorganization in the distribution of the hub nodes has also been found in the multimodal cortical network of schizophrenia (Bassett et al., 2008). Additionally, networks in schizophrenia patients exhibit relatively long physical distances between connected regions, a finding which was compatible with inefficient axonal wiring (Bassett et al., 2008). In the current study, E_{glob} and E_{loc}, rather than the classical path length L and local clustering C, that have been used in previous studies (Liu et al., 2008; Micheloyannis et al., 2006), were used to characterize the small-world behavior in a weighted network. Efficient small-world properties have successfully been estimated for anatomical networks in macaque, cat and healthy human brain cortices (Achard and Bullmore, 2007; Gong et al., 2009b; Latora and Marchiori, 2001; Li et al., 2009). Consistent with other studies (Gong et al., 2009b; Li et al., 2009), efficient small-world properties were also observed in the individual brains of the healthy controls using our network construction method based on diffusion tracking tractography. This further verifies the concept that the human brain can generate and integrate information with high efficiency at both the global and local scales and can maintain a perfect balance between local necessities (fault tolerance) and wide-scope interactions (Latora and Marchiori, 2001). Along this line, the decrease in the E_{glob} suggests a disease-related lowered efficiency of parallel information processing in the brain system in schizophrenia; meanwhile, the unchanged local efficiency suggests a retention of a normal level of fault tolerance in schizophrenia. Given that the efficient small-world model reflects an optimal balance between local

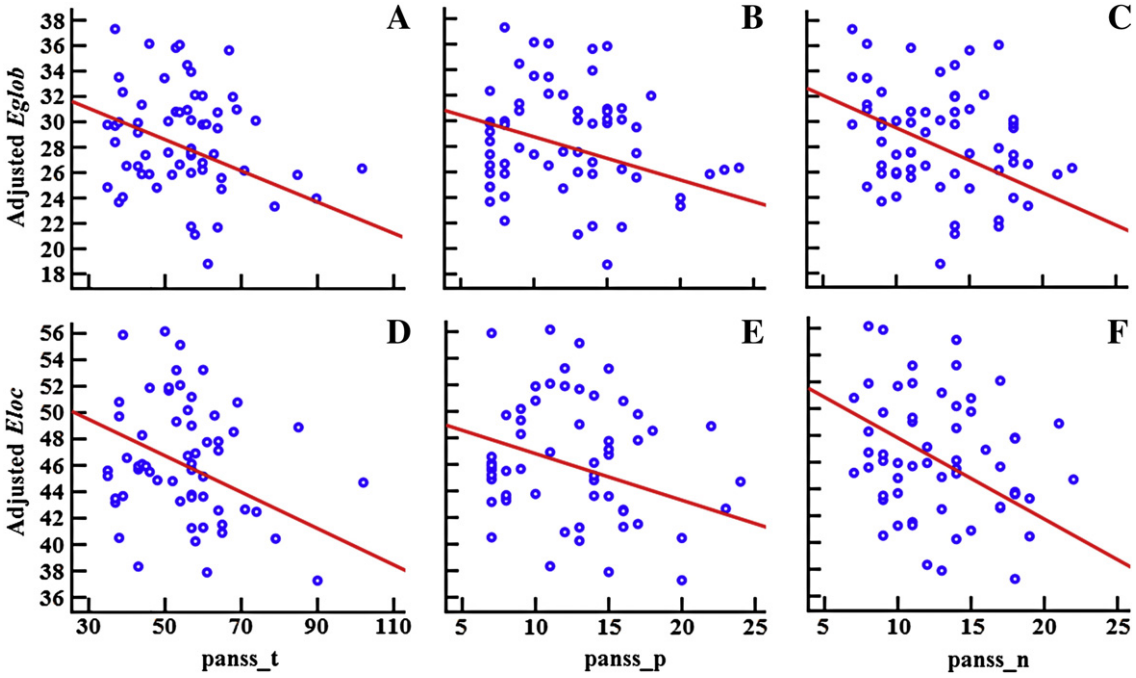

Fig. 4. Partial correlation between the adjusted global or local efficiency and the PANSS scores at a threshold of 6. The results were calculated after adjusting for the effects of gender, age, brain size and HDRS, using a general linear model. Partial correlation between E_{glob} and (A) PANSS_t ($p=0.006$, $pcc=-0.355$), (B) PANSS_p ($p=0.017$, $pcc=-0.308$), (C) PANSS_n ($p=0.007$, $pcc=-0.346$). Partial correlation between E_{loc} and (D) PANSS_t ($p=0.008$, $pcc=-0.340$), (E) PANSS_p ($p=0.042$, $pcc=-0.266$), (F) PANSS_n ($p=0.006$, $pcc=-0.353$). Note: The statistical test of the HDRS variable was performed on 63 patients (16 of the 79 patients had no HDRS variable). The significance threshold was set at $p<0.05$. Abbreviations: please see Table 1, Fig. 1.

specialization and global integration, the decreased E_{glob} combined with comparable values for E_{loc} in the schizophrenia networks indicates a disturbance of the normal balance, which would tend to make information propagation less efficient. Our results thus provide new evidence for the dysconnection hypothesis from the perspective of an anatomical network.

Regional localization of the effects on network efficiency further corroborated the disrupted small-world properties in schizophrenia. The decreased regional efficiency in schizophrenia was found mainly in the frontal associative cortices, the paralimbic/limbic region, and a subcortical structure (the left putamen), most of which have previously been suggested to be anatomically or functionally abnormal in schizophrenia (Kanaan et al., 2005; Kubicki et al., 2007; Kyriakopoulos and Frangou, 2009; Menon et al., 2001; Turetsky et al., 2009). The regional efficiency of each node is a measure of its connectivity to all the other nodes in the network, thus this measure quantifies the importance of the nodes for the communication within the network (Achard and Bullmore, 2007; Gong et al., 2009b). Thus, alterations in the regional efficiency reflect abnormalities in interregional connectivity. The cortical connectivity pattern depends biologically on the axonal properties across the cerebral cortex (Gong et al., 2009b). Many previous studies have reported anatomical connectivity abnormalities that are revealed by an altered FA in the prefrontal regions (Kumra et al., 2004) and the frontal-related white matter tracts, such as the arcuate fasciculus, superior and inferior longitudinal fasciculus (Ashtari et al., 2007; Karlsgodt et al., 2008; Kubicki et al., 2005), as well as in the white matter tracts linking the paralimbic/limbic regions to the associational cortices, such as the cingulum bundle and fornix (Kubicki et al., 2003; Zhou et al., 2008). Thus, a regional change in efficiency in the frontal associative cortices and the paralimbic/limbic regions in schizophrenia, as we observed in this study, should not be unexpected. However, localized neuronal body deficits may also contribute to altered cortical connectivity patterns (Gong et al., 2009b). A decrease in gray matter volume, a reflection of deficits in neuronal bodies that can be detected by imaging, has repeatedly been found in the basal ganglia, including the putamen, in schizophrenia (Lang et al., 2001). This decreased gray matter volume in the putamen may hamper its normal connections and its communication with other regions and may be revealed as a decrease in regional efficiency. The $p<0.01$ significance level for the regional analysis (uncorrected for multiple comparisons) in our current study was relatively low. Therefore the analysis of the regional localization of effects of schizophrenia on network efficiency should be regarded as exploratory in nature. The heterogeneity of the subtypes in our dataset is a potentially confounding factor. An even higher level of significance might be able to be achieved in future studies by including patients with a more homogeneous clinical profile.

An important finding of this study is the significant negative correlation between the topological measurements of the small-world brain anatomical networks and symptom ratings on the PANSS in the schizophrenia patients. That is, the more severe the positive or negative symptoms, the lower the E_{glob} and E_{loc}. When combined with the disrupted efficient small-world properties in the schizophrenia group, this finding strongly suggests that disturbance in the integrative processing of information, as revealed by the disruption of the efficient small-world structure of the brain, is related to deterioration in the symptoms of schizophrenia. This seems obvious; however previous studies which explored the clinical correlations with the topological measurements of the functional network in schizophrenia have not reported meaningful correlations between network structure and symptom ratings based on the PANSS (Liu et al., 2008; Rubinov et al., 2009; van den Heuvel et al., 2010). In these earlier studies, patients with a recent first episode (Rubinov et al., 2009) or with a shorter duration of illness (Liu et al., 2008) were recruited. However, in the present study, patients with a chronic course were also included. This illness chronicity may be an important factor that led to our being able to identify specific associations between symptom profiles and the patterns of dysconnection revealed by the disrupted network properties (Rubinov et al., 2009). The correlation between the topological measures of the anatomical network and the severity of symptoms in schizophrenia leads us to believe that altered anatomical connectivity patterns

underlie the abnormal brain function and clinical symptoms observed in schizophrenia. No significant correlations were found between the network properties and the duration of illness in this study. This may suggest that the duration of illness is independent of the symptom profiles, a finding which is consistent with clinical observations (Loebel et al., 1992).

As a preliminary exploration of the anatomical basis for disruption in the brain small-world network in schizophrenia, the current study enrolled a relatively large sample of patients in order to obtain robust and stable findings. However, the large sample size also may have introduced some potentially confounding factors that need to be considered, such as the effects of medication dosage. In terms of network properties, although one study reported that pharmacological blockade of dopamine D2 receptors by a single dose of sulpiride 400 mg was acutely associated with impaired global and local efficiency of the networks (Achard and Bullmore, 2007), other studies have not found significant correlations between antipsychotic medication dosages and network measurements (Liu et al., 2008; Micheloyannis et al., 2006) or else have found a significantly positive correlation (Rubinov et al., 2009) which was independent of the severity of symptoms in schizophrenia. These clinical studies suggest that medication is unlikely to be a confounding factor and may, on the contrary, exert a 'normalizing' influence and thus argue against a direct treatment effect accounting for the between-group differences. Additionally, subtype heterogeneity may be another potentially confounding factor. Although more definitive conclusions will require unmedicated patients with a homogeneous clinical profile, our stable findings that the efficient small-world properties in the anatomical network were disrupted and deteriorated with a deterioration of symptoms in schizophrenia lead us to believe that anatomical network analysis may be able to play a vital role in improving our understanding of the pathophysiology of schizophrenia and aid researchers in detecting imaging biomarkers for schizophrenia.

Methodological considerations

In our current study, a deterministic tractography method and the *AAL* template were used for network construction. The *AAL* template primarily masks gray matter, but a deterministic tractography algorithm is not applicable in gray matter regions at low FA values. Actually, as some previous articles (Gong et al., 2009a; Li et al., 2009) mentioned, there is a risk that some of the fiber tracts reconstructed using our method may not belong to the specific *AAL* region if an *AAL* mask contained too many white matter voxels that are not truly adjacent to the cortex. As a potential solution for this issue, Gong et al. (2009a) removed white matter voxels in the raw *AAL* cortical mask if no cortical voxels existed within their 2-mm cubic neighborhood. However, their method could lead to another risk, that of excluding the fiber tracts that actually belong to the specific *AAL* region (Li et al., 2009). In the current study, we utilized tracking parameters that were similar to those used in some previous studies (Li et al., 2009; Thottakara et al., 2006); that is, an FA threshold of 0.3 was used for selecting seed voxels to reconstruct fiber tracts originating from different Brodmann areas. According to Li et al. (2009), the FA threshold we used is basically valid for limiting the number of false-positive connections. Fig. S2 in the Supplementary materials shows six well-known white matter fiber tracts from four subjects (2 schizophrenia patients and 2 normal controls) randomly selected from our dataset. These characteristic fiber bundles may indicate that the tracking results are basically credible. A probabilistic tractography method may be a better choice for our future work, as this method is advantageous for overcoming the fiber crossing problem (Behrens et al., 2003, 2007; Lazar and Alexander, 2005). However, in our current study, the DTI images were obtained from a 1.5-T MRI scanner using 13 non-collinear diffusion encoding directions; a single tensor model and deterministic tracking method might be the optimal choice.

That the E_{glob} did not change much as the threshold increased and the networks got sparser (Fig. 1A), while the E_{loc} became even higher (Fig. 1B) seems counterintuitive. We think this result is rational due to the use of a dissimilarity link weight in the current study. Specifically, as the threshold increased, the edges with higher weights (corresponding to a lower number of fiber bundles between nodes and a longer distance) were removed first; these edges were usually not on the shortest pathway between regions, hence the elimination of these "ineffective" edges contributed little to the E_{glob} but enhanced the E_{loc} of the whole network. However, the efficiency would decrease anyway as the threshold continued to increase. Fig. S3 shows the entire variation trend ofE_{glob} andE_{loc} over a larger threshold range (from 1 to 50). Interestingly, as the weighted network degenerated to a binary network, E_{glob} andE_{loc} both decreased monotonously as the threshold increased (Fig. S4 in Supplementary materials).

Additionally, regions on the *AAL* template differ in size, which may have a confounding effect on the link weight of the network nodes. Furthermore, the definition of the template (*i.e.* the inclusion and exclusion of some brain regions) could also affect the statistical results. However, understanding how to assess and control these influence remains an open question. In the current study, we are mainly concerned with differences in network attributes between healthy and schizophrenia groups. To test the between-group region size differences, we performed a two-tailed *t*-test on each pair of corresponding brain region and found no significant result ($p<0.05$). This result suggests that region sizes have equivalent influences in both the healthy and schizophrenia groups and, therefore, contribute little to the between-group differences we found in the current study. Nevertheless, further investigations will be necessary to better address the methodological limitations of our current study.

Conclusions

Our findings provide direct evidence for a disrupted anatomical network in schizophrenia and suggest a structural basis for the dysconnection manifested by disrupted small-world functional networks. Correlations between topological measures of efficient small-world properties and the severity of symptoms in schizophrenia lead us to believe that altered global architecture of the anatomical connectivity patterns underlie the abnormal brain function and clinical symptoms observed in schizophrenia.

Funding

This work was supported by the National Key Basic Research and Development Program (973) (Grant Number 2011CB707800) to Dr Jiang; the Natural Science Foundation of China (Grant Number 30730035 to Dr Jiang, Grant Number 30900487 to Dr. Zhou); Ministry of Economic Affairs (Grant Number 98-EC-17-A-19-S2-0103); National Health Research Institute (Grant Number NHRI-EX98-9813EC); and National Science Council (Grant Numbers 98-2517-S-004-001-MY3 and 98-2627-B-010-008)

Acknowledgments

The authors acknowledge MR support from the MRI Core Laboratory, NYMU and support from the Ministry of Education (Aim for the Top University Plan). The authors thank Drs. Edmund F. and Rhoda E. Perozzi for English editing assistance and discussions. The authors thank Dr. Yong Liu for his valuable suggestions on the revised manuscript. The authors are grateful to Professor Godfrey Pearlson for his constructive comments and suggestions.

Appendix A. Supplementary data

Supplementary data to this article can be found online at doi:10.1016/j.neuroimage.2011.09.035.

References

Achard, S., Bullmore, E., 2007. Efficiency and cost of economical brain functional networks. PLoS Comput. Biol. 3, e17.

Andreasen, N.C., Nopoulos, P., O'Leary, D.S., Miller, D.D., Wassink, T., Flaum, M., 1999. Defining the phenotype of schizophrenia: cognitive dysmetria and its neural mechanisms. Biol. Psychiatry 46, 908–920.

Ashtari, M., Cottone, J., Ardekani, B.A., Cervellione, K., Szeszko, P.R., Wu, J., Chen, S., Kumra, S., 2007. Disruption of white matter integrity in the inferior longitudinal fasciculus in adolescents with schizophrenia as revealed by fiber tractography. Arch. Gen. Psychiatry 64, 1270–1280.

Bai, Y.M., Chou, K.H., Lin, C.P., Chen, I.Y., Li, C.T., Yang, K.C., Chou, Y.H., Su, T.P., 2009. White matter abnormalities in schizophrenia patients with tardive dyskinesia: a diffusion tensor image study. Schizophr. Res. 109, 167–181.

Bassett, D.S., Bullmore, E., Verchinski, B.A., Mattay, V.S., Weinberger, D.R., Meyer-Lindenberg, A., 2008. Hierarchical organization of human cortical networks in health and schizophrenia. J. Neurosci. 28, 9239–9248.

Bassett, D.S., Bullmore, E.T., Meyer-Lindenberg, A., Apud, J.A., Weinberger, D.R., Coppola, R., 2009. Cognitive fitness of cost-efficient brain functional networks. Proc. Natl. Acad. Sci. U. S. A. 106, 11747–11752.

Behrens, T.E., Johansen-Berg, H., Woolrich, M.W., Smith, S.M., Wheeler-Kingshott, C.A., Boulby, P.A., Barker, G.J., Sillery, E.L., Sheehan, K., Ciccarelli, O., Thompson, A.J., Brady, J.M., Matthews, P.M., 2003. Non-invasive mapping of connections between human thalamus and cortex using diffusion imaging. Nat. Neurosci. 6, 750–757.

Behrens, T.E., Berg, H.J., Jbabdi, S., Rushworth, M.F., Woolrich, M.W., 2007. Probabilistic diffusion tractography with multiple fibre orientations: what can we gain? NeuroImage 34, 144–155.

Boutillier, A.L., Macedo, C.E., Angst, M.J., Sandner, G., 2008. How can we justify the use of lower animal models to understand the pathophysiology of schizophrenia? Advances in Cognitive Neurodynamics. Springer, pp. 577–582.

Bullmore, E., Sporns, O., 2009. Complex brain networks: graph theoretical analysis of structural and functional systems. Nat. Rev. Neurosci. 10, 186–198.

Bullmore, E.T., Frangou, S., Murray, R.M., 1997. The dysplastic net hypothesis: an integration of developmental and dysconnectivity theories of schizophrenia. Schizophr. Res. 28, 143–156.

Friston, K.J., 1998. The disconnection hypothesis. Schizophr. Res. 30, 115–125.

Gong, G., He, Y., Concha, L., Lebel, C., Gross, D.W., Evans, A.C., Beaulieu, C., 2009a. Mapping anatomical connectivity patterns of human cerebral cortex using in vivo diffusion tensor imaging tractography. Cereb. Cortex 19, 524–536.

Gong, G., Rosa-Neto, P., Carbonell, F., Chen, Z.J., He, Y., Evans, A.C., 2009b. Age- and gender-related differences in the cortical anatomical network. J. Neurosci. 29, 15684–15693.

Hagmann, P., Kurant, M., Gigandet, X., Thiran, P., Wedeen, V.J., Meuli, R., Thiran, J.P., 2007. Mapping human whole-brain structural networks with diffusion MRI. PLoS One 2, e597.

Hagmann, P., Cammoun, L., Gigandet, X., Meuli, R., Honey, C.J., Wedeen, V.J., Sporns, O., 2008. Mapping the structural core of human cerebral cortex. PLoS Biol. 6, e159.

Hamilton, M., 1960. A rating scale for depression. J. Neurol. Neurosurg. Psychiatry 23, 56–62.

Iturria-Medina, Y., Sotero, R.C., Canales-Rodriguez, E.J., Aleman-Gomez, Y., Melie-Garcia, L., 2008. Studying the human brain anatomical network via diffusion-weighted MRI and Graph Theory. NeuroImage 40, 1064–1076.

Kanaan, R.A., Kim, J.S., Kaufmann, W.E., Pearlson, G.D., Barker, G.J., McGuire, P.K., 2005. Diffusion tensor imaging in schizophrenia. Biol. Psychiatry 58, 921–929.

Karlsgodt, K.H., van Erp, T.G., Poldrack, R.A., Bearden, C.E., Nuechterlein, K.H., Cannon, T.D., 2008. Diffusion tensor imaging of the superior longitudinal fasciculus and working memory in recent-onset schizophrenia. Biol. Psychiatry 63, 512–518.

Kay, S.R., Flszbein, A., Opler, L.A., 1987. The positive and negative syndrome scale (PANSS) for schizophrenia. Schizophr. Bull. 13, 261–276.

Kubicki, M., Westin, C.F., Nestor, P.G., Wible, C.G., Frumin, M., Maier, S.E., Kikinis, R., Jolesz, F.A., McCarley, R.W., Shenton, M.E., 2003. Cingulate fasciculus integrity disruption in schizophrenia: a magnetic resonance diffusion tensor imaging study. Biol. Psychiatry 54, 1171–1180.

Kubicki, M., Park, H., Westin, C.F., Nestor, P.G., Mulkern, R.V., Maier, S.E., Niznikiewicz, M., Connor, E.E., Levitt, J.J., Frumin, M., Kikinis, R., Jolesz, F.A., McCarley, R.W., Shenton, M.E., 2005. DTI and MTR abnormalities in schizophrenia: analysis of white matter integrity. NeuroImage 26, 1109–1118.

Kubicki, M., McCarley, R., Westin, C.F., Park, H.J., Maier, S., Kikinis, R., Jolesz, F.A., Shenton, M.E., 2007. A review of diffusion tensor imaging studies in schizophrenia. J. Psychiatr. Res. 41, 15–30.

Kumra, S., Ashtari, M., McMeniman, M., Vogel, J., Augustin, R., Becker, D.E., Nakayama, E., Gyato, K., Kane, J.M., Lim, K., Szeszko, P., 2004. Reduced frontal white matter integrity in early-onset schizophrenia: a preliminary study. Biol. Psychiatry 55, 1138–1145.

Kyriakopoulos, M., Frangou, S., 2009. Recent diffusion tensor imaging findings in early stages of schizophrenia. Curr. Opin. Psychiatry 22, 168–176.

Lang, D.J., Kopala, L.C., Vandorpe, R.A., Rui, Q., Smith, G.N., Goghari, V.M., Honer, W.G., 2001. An MRI study of basal ganglia volumes in first-episode schizophrenia patients treated with risperidone. Am. J. Psychiatry 158, 625–631.

Latora, V., Marchiori, M., 2001. Efficient behavior of small-world networks. Phys. Rev. Lett. 87, 198701.

Latora, V., Marchiori, M., 2003. Economic small-world behavior in weighted networks. Eur. Phys. J. B 32, 249–263.

Lazar, M., Alexander, A.L., 2005. Bootstrap white matter tractography (BOOT-TRAC). NeuroImage 24, 524–532.

Li, Y., Liu, Y., Li, J., Qin, W., Li, K., Yu, C., Jiang, T., 2009. Brain anatomical network and intelligence. PLoS Comput. Biol. 5, e1000395.

Liu, Y., Liang, M., Zhou, Y., He, Y., Hao, Y., Song, M., Yu, C., Liu, H., Liu, Z., Jiang, T., 2008. Disrupted small-world networks in schizophrenia. Brain 131, 945–961.

Loebel, A.D., Lieberman, J.A., Alvir, J.M., Mayerhoff, D.I., Geisler, S.H., Szymanski, S.R., 1992. Duration of psychosis and outcome in first-episode schizophrenia. Am. J. Psychiatry 149, 1183–1188.

Madden, D.J., Whiting, W.L., Huettel, S.A., White, L.E., MacFall, J.R., Provenzale, J.M., 2004. Diffusion tensor imaging of adult age differences in cerebral white matter: relation to response time. NeuroImage 21, 1174–1181.

Menon, V., Anagnoson, R.T., Glover, G.H., Pfefferbaum, A., 2001. Functional magnetic resonance imaging evidence for disrupted basal ganglia function in schizophrenia. Am. J. Psychiatry 158, 646–649.

Micheloyannis, S., Pachou, E., Stam, C.J., Breakspear, M., Bitsios, P., Vourkas, M., Erimaki, S., Zervakis, M., 2006. Small-world networks and disturbed functional connectivity in schizophrenia. Schizophr. Res. 87, 60–66.

Mori, S., Crain, B.J., Chacko, V.P., van Zijl, P.C., 1999. Three-dimensional tracking of axonal projections in the brain by magnetic resonance imaging. Ann. Neurol. 45, 265–269.

Rubinov, M., Knock, S.A., Stam, C.J., Micheloyannis, S., Harris, A.W., Williams, L.M., Breakspear, M., 2009. Small-world properties of nonlinear brain activity in schizophrenia. Hum. Brain Mapp. 30, 403–416.

Salvador, R., Suckling, J., Coleman, M.R., Pickard, J.D., Menon, D., Bullmore, E., 2005. Neurophysiological architecture of functional magnetic resonance images of human brain. Cereb. Cortex 15, 1332–1342.

Skudlarski, P., Jagannathan, K., Anderson, K., Stevens, M.C., Calhoun, V.D., Skudlarska, B.A., Pearlson, G., 2010. Brain connectivity is not only lower but different in schizophrenia: a combined anatomical and functional approach. Biol. Psychiatry 68, 61–69.

Sporns, O., Chialvo, D.R., Kaiser, M., Hilgetag, C.C., 2004. Organization, development and function of complex brain networks. Trends Cogn. Sci. 8, 418–425.

Stam, C.J., Reijneveld, J.C., 2007. Graph theoretical analysis of complex networks in the brain. Nonlinear Biomed. Phys. 1, 3.

Stephan, K.E., Baldeweg, T., Friston, K.J., 2006. Synaptic plasticity and dysconnection in schizophrenia. Biol. Psychiatry 59, 929–939.

Thottakara, P., Lazar, M., Johnson, S.C., Alexander, A.L., 2006. Application of Brodmann's area templates for ROI selection in white matter tractography studies. NeuroImage 29, 868–878.

Turetsky, B.I., Hahn, C.G., Borgmann-Winter, K., Moberg, P.J., 2009. Scents and nonsense: olfactory dysfunction in schizophrenia. Schizophr. Bull. 35, 1117–1131.

Tzourio-Mazoyer, N., Landeau, B., Papathanassiou, D., Crivello, F., Etard, O., Delcroix, N., Mazoyer, B., Joliot, M., 2002. Automated anatomical labeling of activations in SPM using a macroscopic anatomical parcellation of the MNI MRI single-subject brain. NeuroImage 15, 273–289.

van den Heuvel, M.P., Mandl, R.C., Stam, C.J., Kahn, R.S., Hulshoff Pol, H.E., 2010. Aberrant frontal and temporal complex network structure in schizophrenia: a graph theoretical analysis. J. Neurosci. 30, 15915–15926.

Watts, D.J., Strogatz, S.H., 1998. Collective dynamics of 'small-world' networks. Nature 393, 440–442.

Zalesky, A., Fornito, A., Seal, M.L., Cocchi, L., Westin, C.F., Bullmore, E.T., Egan, G.F., Pantelis, C., 2010. Disrupted axonal fiber connectivity in schizophrenia. Biol. Psychiatry 69, 80–89.

Zhou, Y., Shu, N., Liu, Y., Song, M., Hao, Y., Liu, H., Yu, C., Liu, Z., Jiang, T., 2008. Altered resting-state functional connectivity and anatomical connectivity of hippocampus in schizophrenia. Schizophr. Res. 100, 120–132.